doi:10.1017/S1431927622007048
Microsc. Microanal. 28 (Suppl 1), 2022

In-situ Lorentz Imaging of Room-Temperature Ferromagnetic Domains in Monolayer Vanadium-Doped WS_2

Ariana Ray[1], Mingzu Liu[2], Boyang Zheng[2], Da Zhou[2], Vincent H. Crespi[2], Mauricio Terrones[2] and David A. Muller[1*].

[1.] Cornell University, School of Applied and Engineering Physics, Ithaca, NY, USA.
[2.] Pennsylvania State University, Department of Physics, University Park, PA, USA.
* Corresponding author: david.a.muller@cornell.edu

Substitutional hole doping of monolayer WS_2 with vanadium atoms has recently been demonstrated to induce long-range, room-temperature ferromagnetic ordering [1]. These dilute magnetic semiconductors formed from doped transition metal dichalcogenides, such as V-doped WS_2, are a new class of air-stable, intrinsic magnetic materials with promising spintronics applications [2]. However, their local magnetic domain structures have not been explored in detail, in part because of the extreme difficulty of detecting magnetic signals from monolayers in Lorentz TEM. Here we image magnetic domains and their corresponding atomic lattice in monolayer WS_2 for a range of vanadium dopant concentrations using Lorentz TEM and atomic-resolution STEM. We find that the material is not uniformly magnetized but contains micron-sized monolayer ferromagnetic domains with an in-plane easy axis and a saturation field of ~50 mT. This is, we believe, the first reported imaging of a monolayer magnet with Lorentz TEM.

The crystal structure and a high-angle annular dark field (HAADF) STEM image of V-doped WS_2 are shown in Fig. 1a-b, where the vanadium dopants appear as dark spots in the bright tungsten lattice. While monolayer WS_2 is not magnetic, the sparse substitution of tungsten sites with vanadium atoms hole dopes the material and creates a spin-polarized impurity state in the band structure, leading to long-range ferromagnetic ordering [1]. The strength of the magnetism is sensitive to the amount and distribution of the dopant atoms, suggesting the possibility of tunable magnetism given sufficient control over the vanadium doping [1]. It is important to note that the process of S/TEM imaging, which is known to create sulfur vacancies that electron-dope the WS_2 [3], may counteract the vanadium-induced hole doping needed to create the magnetic ordering.

Given the extreme sensitivity of the dopant-induced magnetism to radiation-induced defects and charging in the monolayer materials, we first survey the films with low-dose (~0.3 $e^-/Å^2$), low-magnification Lorentz TEM. Lorentz TEM images are sensitive to in-plane ferromagnetic domain boundaries and discontinuities. An in-plane sample magnetization causes the incident electron beam to deflect due to the Lorentz force. When a defocused probe is used to enhance the phase contrast, the difference in the beam deflection directions at a domain boundary causes a bright or dark line to appear there. Antiferromagnetic and out-of-plane ferromagnetic domains, which cause no net beam deflection, do not produce Lorentz TEM contrast.

An in-plane ferromagnetic domain in monolayer 2% V-doped WS_2 is shown in Figure 2. Lorentz TEM images taken at a defocus of –3 mm in Fig. 2b show the contrast evolution of a monolayer V-WS_2 flake on a silicon nitride window as the applied out-of-plane magnetic field (B_{ext}) is varied in a loop between positive and negative fields of ~ ±100 mT, which saturates the magnetization. An image of the flake at saturation has been subtracted to remove electrostatic contributions. At B_{ext} = 0, strong domain boundary contrast is seen along the WS_2 flake edge, where the in-plane magnetization is spatially discontinuous. As B_{ext} is swept to large positive and negative values, the magnetization rotates out-of-plane to align with the external field, and the domain boundary contrast disappears. A plot of the integrated domain boundary intensity vs. applied field in Fig. 2c confirms the cyclic field-dependent contrast and an in-plane easy axis, with maximum domain contrast at $B_{ext} = 0$ and near-zero contrast when $|B_{ext}|$ is greater than a saturation field of ~50 mT. The macroscopic in-plane ferromagnetic hysteresis loop (Fig. 2d) on a similar 2% V-doped monolayer sample supports our LTEM results, indicating we have been able to not only detect but also reproduce the macroscopic field response in microscopic detail for a single-monolayer-thick material [4].

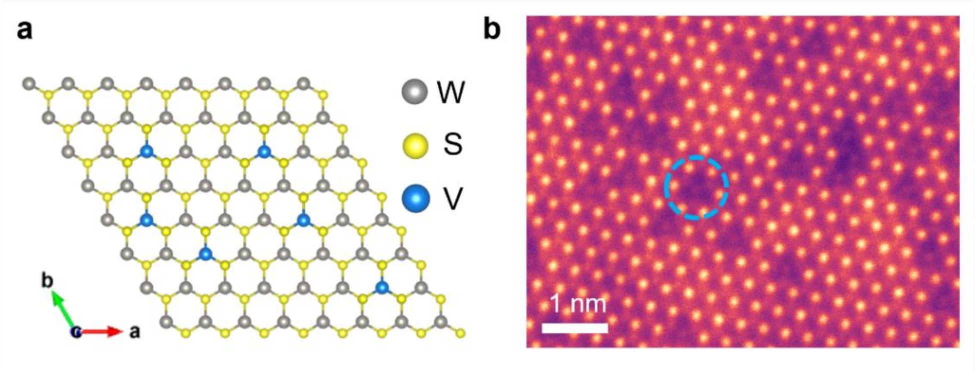

Figure 1: Monolayer V-doped WS_2 lattice. (a) Crystal structure of monolayer WS_2 with substitutional vanadium-doping at the tungsten sites (blue atoms). **(b)** HAADF image of monolayer V-doped WS_2 taken at 60 kV, showing darker vanadium atoms (ex: blue circle) interspersed among the bright tungsten atoms.

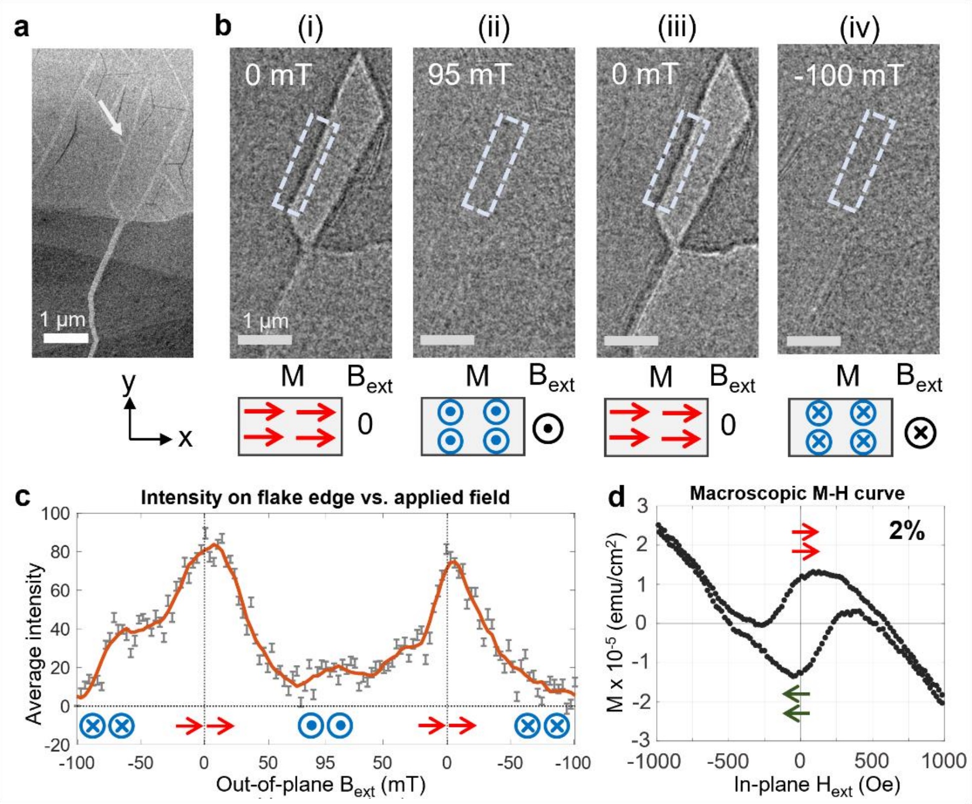

Figure 2: In-plane ferromagnetic domain in monolayer 2% V-doped WS$_2$. (a) TEM image of monolayer flake (see arrow). **(b)** Lorentz TEM domain contrast on flake edge (dashed rectangle) appearing and disappearing as the out-of-plane magnetic field (B_{ext}) is looped between –100 mT to 95 mT. Saturated image at –100 mT is subtracted to remove electrostatic contrast. As illustrated below each sub-panel, the sample's magnetization is in-plane at zero field (i, ii) and has rotated to fully align with the out-of-plane external field at ~ ±100 mT (iii, iv). Our observation of an in-plane ferromagnetic domain is confirmed by the integrated domain-boundary intensity vs. applied field **(c)**, which shows maximum domain contrast at $B_{ext} = 0$ and roughly constant intensity beyond the saturation field of ±50 mT. This result is supported by the macroscopic in-plane ferromagnetic hysteresis loop in **(d)** (Adapted from [1]).

References:

[1] F Zhang et al., Adv. Sci. **7** (2020), p. 2001174. doi:10.1002/advs.202001174
[2] A Hirohata et al., Journal of Magnetism and Magnetic Materials **509** (2020). doi:10.1016/j.jmmm.2020.166711
[3] S Wang, A Robertson and J H Warner, Chem. Soc. Rev. **47** (2018), p. 6764. doi:10.1039/cBcs00236c

[4] The authors acknowledge funding from the National Science Foundation MRSEC and MIP programs (DMR-1719875, DMR-2039351, DMR- 2039380), and the AFOSR (FA9550-18-1-0072).